Published in final edited form as:
Biomech Model Mechanobiol. 2014 June ; 13(3): 565–572. doi:10.1007/s10237-013-0518-8.

Strain-Dependent Oxidant Release in Articular Cartilage Originates from Mitochondria

Brouillette M J[1,2], **Ramakrishnan P S**[1,2], **Wagner V M**[1,2], **Sauter E E**[1,2], **Journot B J**[1,2], **McKinley T O**[1], and **Martin J A**[1,2]

[1]Department of Orthopaedics and Rehabilitation, University of Iowa, Iowa City

[2]Department of Biomedical Engineering, University of Iowa, Iowa City

Abstract

Mechanical loading is essential for articular cartilage homeostasis and plays a central role in the cartilage pathology, yet the mechanotransduction processes that underlie these effects remain unclear. Previously we showed that lethal amounts of reactive oxygen species (ROS) were liberated from the mitochondria in response to mechanical insult, and that chondrocyte deformation may be a source of ROS. To this end, we hypothesized that mechanically-induced mitochondrial ROS is related to the magnitude of cartilage deformation. To test this, we measured axial tissue strains in cartilage explants subjected to semi-confined compressive stresses of 0, 0.05, 0.1, 0.25, 0.5, or 1.0 MPa. The presence of ROS was then determined by confocal imaging with dihydroethidium (DHE), an oxidant sensitive fluorescent probe. Our results indicated that ROS levels increased linearly relative to the magnitude of axial strains ($r^2 = 0.83$, $p < 0.05$), and significant cell death was observed at strains > 40%. By contrast, hydrostatic stress, which causes minimal tissue strain, had no significant effect. Cell permeable superoxide dismutase mimetic Mn(III)tetrakis (1-methyl-4-pyridyl) porphyrin pentachloride (MnTMPyP) significantly decreased ROS levels at 0.5 and 0.25 MPa. Electron transport chain inhibitor, rotenone, and cytoskeletal inhibitor, cytochalasin B, significantly decreased ROS levels at 0.25 MPa. Our findings strongly suggest that ROS and mitochondrial oxidants contribute to cartilage mechanobiology.

Keywords

Cartilage; Chondrocyte; Reactive Oxygen Species (ROS); Superoxide; Mechanical Loading; Static Stress; Hydrostatic Stress; Cytoskeleton

1. Introduction

The material properties of articular cartilage are tailored to transmit physiological loads across the joint and to provide necessary articulation for joint motion. Physical forces experienced in the joint strongly influence the metabolic response of resident chondrocytes that in turn facilitate functional adaptation of cartilage for future mechanical demands (Wong and Carter 2003). Although unclear, there is evidence to suggest that chondrocyte

Corresponding Author: Marc J Brouillette, Graduate Research Assistant, Ignacio Ponseti Orthopaedic Cell Biology Lab, Department of Orthopaedics and Rehabilitation, University of Iowa, Iowa City, marc-brouillette@uiowa.edu 1-319-335-7550.

deformation in response to mechanical load on cartilage initiates specific intracellular processes that alter cellular viability, matrix synthesis and inflammation (Quinn et al. 1998; Quinn et al. 2001; Stevens et al. 2009; Torzilli et al. 2006).

Cartilage is a hypoxic tissue, where mitochondria are scarce and ATP production occurs almost exclusively through anaerobic glycolysis (Stockwell 1991; Otte 1991). Although the number of mitochondria in cartilage is low, their dysfunction has been correlated with the development of osteoarthritis (Cillero-Pastor et al. 2008; Blanco et al. 2011), suggesting that they may be contributing to cartilage homeostasis and pathology.

In highly oxygenated tissues, it is estimated that 2-3% of molecular oxygen is incompletely reduced to ROS in the mitochondria, specifically superoxide ($O_2^{\bullet -}$) (Chance and Williams 1955). This level is sufficient for intracellular signaling and other physiological processes without causing extensive oxidative damage (Chance and Williams 1955). Previous experiments demonstrated that cartilage requires a source of oxidants to maintain glycolytic ATP synthesis (Lee and Urban 2002), and that mitochondrial oxidants act as this source in low oxygen conditions (Martin et al. 2012). Interestingly, superoxide can be targeted and quenched intracellularly using a cell-permeable superoxide dismutase mimetic, such as MnTMPyP. This chemical converts superoxide to hydrogen peroxide and can grant protection from mitochondrial superoxide related damage (Strathmann et al. 2010).

Mechanical stimulation of chondrocytes has been shown to reorganize the cytoskeleton (Durrant et al. 1999) and even distort the mitochondria (Knight et al. 2006). This mechanical distortion has been linked to mitochodrial ROS release, which is dependent on the condition of the cytoskeleton. By dissolving the chondrocyte cytoskeleton with cytochalasin B, using rotenone to block complex I of the electron transport chain, or sequestering ROS with the antioxidant N-acetyl cysteine we were able to reduce the amount of ROS and cell death, indicating that mitochondria are involved in chondrocyte mechanotransduction, and cytoskeletal deformation was coupled to this lethal mitochondrial ROS release (Martin et al. 2009; Goodwin et al. 2010; Sauter et al. 2012).

Taken together, these studies led us to hypothesize that mitochondrial production of ROS, specifically superoxide, is a deformation-dependent, cytoskeleton-mediated process. Using a bovine osteochondral explant model, we subjected specimens to either semi-confined static compressive stresses or hydrostatic stresses between 0 and 1.0 MPa. ROS production and chondrocyte viability were assessed using confocal microscopy and compared to axial tissue strains. The effects of MnTMPyP, cytochalasin B, or rotenone to sequester superoxide, dissolve the cytoskeleton, or block mitochondrial complex I, respectively, were determined in a static compressive stress model.

2. Methods

2.1. Explant Harvest and Culture

Osteochondral explants (15mm × 15mm) were harvested from mature bovine lateral tibial plateaus under sterile conditions. The subchondral bone was left attached with a thickness of 5-8mm. The explants were then allowed to equilibrate in culture media containing 45%

Dulbecco's Modified Essential Medium (DMEM), 45% F12, 10% Fetal Bovine Serum (Invitrogen) in low oxygen (5% O_2, 5% CO_2) for 48 hours.

2.2. Mechanical Loading

2.2.1. Compressive Stress Apparatus—Mechanical loading was achieved using a custom indentation device previously described (Ramakrishnan et al. 2011) (Fig 1a) that was housed inside a low oxygen incubator (5% O_2, 5% CO_2). Prior to loading, central specimen thickness was measured using a calibrated ultrasound device (Fig S1, Sonopen®, Olympus NDT). Specimens were securely fixed in a custom jig interfaced with stainless steel screw fixators with the explant completely bathed low oxygen equilibrated media. Specimens were loaded with an 8.0 mm-diameter flat, non-porous cylindrical indenter. The indenter was brought into contact with a specimen to a minimal tare load of 0.1N. Immediately after reaching the tare load, specimens were loaded at a constant strain rate of 0.1/s until the target stress was achieved (0.05, 0.1, 0.25, 0.5, or 1.0MPa). The target stress was then held constant for one hour while actuator displacement was recorded. Axial strain was calculated as a ratio of maximal displacement after one hour of loading and cartilage thickness prior to loading (it was assumed that there was no deformation in the subchondral bone).

2.2.2. Hydrostatic Stress Apparatus—Cartilage explants were placed inside impermeable bags, completely bathed in low oxygen equilibrated media, heat-sealed, and placed inside the hydrostatic chamber. The chamber was evacuated and filled with distilled water to function as the pressurizing liquid. The hydrostatic pressure chamber was instrumented with a stepper motor (Ultramotion®, with optical encoder feedback) and pressure transducer (Sensotec® FP2000 series). Static pressure was achieved using the stepper motor to depress a hydraulic piston attached to the chamber (Fig 1b). Actuator control and pressure feedback were controlled and programmed with LabVIEW. Specimens were subjected to one hour of constant hydrostatic stress.

2.3. Imaging of Oxidants, Viability and Quantification

2.3.1. Confocal Imaging—Immediately after loading, explants were stained with 5.0μM dihydroethidium (DHE, Invitrogen), an ROS indicator, or 1.0μM ethidium homodimer-2 (EthD-2, Invitrogen), a cell death indicator, along with 1.0μM Calcein-AM (Invitrogen), a live cell indicator, for 30 minutes under previously described culture conditions (Goodwin et al. 2010; Martin et al. 2012). Specimens were imaged using a Bio-Rad MRC-1024 confocal microscope. Images of the explants were made with a 20× water immersion lens (Nikon). Three random sites within the central 4.0 mm of the loaded region (to avoid edge artifacts from loading) were imaged from the surface to a depth of ~200μm in 20μm intervals.

2.3.2. Automated Quantification—Cell counts for oxidant production and viability were achieved using Quantitative Cell Image Processing (QCIP™), a custom automated MATLAB® cell counting program. For any explant, the three image sites were processed for the percentage of DHE or EthD-2 stained cells. The mean percentage for each explant was taken for analysis. Validation and further information on QCIP™ can be found in the supplementary information.

2.4. Effect of Semi-confined Static Compressive Stress on ROS Production and Chondrocyte Viability

Explants were subjected to semi-confined static compressive stress of 0, 0.05, 0.1, 0.25, 0.50, or 1.0 MPa (n=7, 5, 5, 6, 5, 5 respectively) for one hour as described above. Axial strain was calculated as described. Specimens were bathed in Calcein-AM and DHE immediately after loading for 30 minutes. Image data were processed for oxidant and total cell counts using QCIP™. The total number of cells was considered the aggregate of DHE and Calcein-AM positive cells. Oxidant producing cell counts were reported as the mean percentage of the three image sites.

Subsequently, another group explants were subjected the same envelope of compressive stresses, 0, 0.05, 0.1, 0.25, 0.5, or 1.0MPa (n=7, 5, 6, 5, 7, 5 respectively), for one hour and stained with Calcein-AM and EthD-2 after loading. Image data were processed for dead cell and total cell counts using QCIP™. Cell death cell counts were reported as the mean percentage of the three image sites counted (Calcein-AM and EthD-2 pooled for each image).

2.5. Effect of Hydrostatic Stress on ROS Production and Cell Death

Explants were subjected to either 0.5 or 1.0 MPa of hydrostatic stress as described above for one hour. Calcein-AM and DHE (0.5MPa n=5, 1.0MPa n=6) were used to measure oxidant production and Calcein-AM and EthD-2 (0.5MPa n=5, 1.0MPa n=5) used for cell death. ROS production and dead cell count were collected and processed as described above.

2.6. Effect of Inhibitors on ROS Production

To determine if superoxide was the major source of ROS, explants were incubated with 100μM MnTMPyP (Cayman Chemical) for one hour prior to loading. Subsequently specimens were subjected to either 0.25MPa (n=5) or 0.5MPa (n=5) static semi-confined compressive stress for 1 hour with continued exposure to MnTMPyP. Specimens were stained and imaged for ROS production in the same manner as above.

To determine if blocking mitochondrial NADH dehydrogenase (Complex I) during cartilage compression stress had an effect on ROS production, explants were incubated with 2.5μM rotenone (Sigma Aldrich) for one hour prior to loading. Specimens were subjected to either 0.25MPa (n=5) or 0.5MPa (n=5) static semi-confined compressive stress for 1 hour with continued exposure to rotenone. Specimens were stained and imaged for ROS production as described above.

To investigate the role of the cytoskeleton in mitochondrial ROS production, explants were pre-treated with 20μM cytochalasin B (Sigma Aldrich) for four hours prior to loading. Subsequently, specimens were subjected to semi-confined static compressive stress of either 0.25 (n=5) or 0.5 MPa (n=6) for one hour as described. Specimens were stained and imaged for ROS production as previously described.

MnTMPyP, rotenone, and cytochalasin B were not found to be cytotoxic or induce DHE staining in unstressed specimens at the doses and durations used (data not shown) (Sauter et al. 2012; Goodwin et al. 2010; Wolff et al. 2013).

2.7. Statistical Analysis

For all data representation and analyses the mean percentage of DHE (ROS) or EthD-2 (cell death) from the three images for each explant was treated as one data point. The one way ANOVA with Tukey's post hoc test was employed to assess the statistical differences in the staining percentages under the differing stress levels (0, 0.05, 0.1, 0.25, 0.5, or 1.0MPa), with the independent variable being the stress level and the dependent variable being the percentage of DHE or dead cells. Linear Regression and Spearman rank order correlation were also employed to identify the association of tissue strain with the staining percentages (Sigmaplot 11).

To assess the statistical difference between hydrostatic stress and compressive stress, an unpaired t-test was used comparing the hydrostatic stress (0.5MPa, or 1.0MPa) to its corresponding static stress (0.5MPa, or 1.0MPa) for the percentage of DHE stained cells or cell death. A second unpaired t-test was then used to assess statistical significance between each of the hydrostatic stress groups and the unloaded control group.

To assess the statistical difference among pretreatment of MnTMPyP, rotenone, or cytochalasin B on the percentage of DHE stained cells at 0.5MPa or 0.25MPa the one way ANOVA with Tukey's post hoc test was employed at each stress level separately. Here, the independent variable was considered the pretreatment substance (MnTMPyP, rotenone, or cytochalasin B) and the dependent variable was the percentage of DHE stained cells.

3. Results

Representative confocal images from an unloaded control and specimens loaded at all four stress levels show Calcein-AM and DHE staining after static compression (Fig 2). The percentage of DHE-stained cells increased with increasing semi-confined static compressive stress (Fig 3). In unloaded specimens, 2.7% (±4%) of the cells were stained with DHE. ROS-positive DHE staining increased to 5.9% (±3%) at 0.05MPa, 11.1% (±7%) at 0.1 MPa, 35.6% (±17%) at 0.25 MPa, 56.4% (±7%) at 0.5 MPa, and 76.7% (±5%) at 1 MPa. The increases at 0.25, 0.5, and 1.0 MPa were significant ($p<0.05$) over the unloaded control. In contrast, semi-confined static compressive stresses up to 0.5 MPa did not cause widespread chondrocyte death, ranging from 4.1% (±3%) in unloaded specimens to 12.5% (±8%) in specimens loaded up to 0.5 MPa. Chondrocyte death increased significantly ($p<0.05$) in specimens loaded to 1.0 MPa compared to unloaded samples, increasing to 38% (±7%).

Regression analysis revealed a strong linear relationship between axial-tissue compressive strain and DHE staining ($R^2=0.87$, Fig 4a) and the Spearman rank order test showed a positive correlation (0.916; $p<0.001$). In this model, axial-tissue strain best correlated with ROS production. Chondrocytes death, however, had an exponential correlation ($R^2=0.62$, Fig 4b). Strains below 40% caused very little chondrocyte death in contrast to strains above 60% which led to widespread chondrocyte death. The sharp rise in chondrocyte death occurred between 40% and 60% axial-tissue strain.

In contrast to semi-confined compressive stress, hydrostatic stress, which has been shown to induce no bulk tissue strain (Bachrach et al. 1998), did not provoke significant ROS

production at 0.5 MPa (5.4% ±9%) and 1.0 MPa (7.1% ±8%) compared to unloaded specimens (4.1% ±3%) (Fig 3). Likewise, hydrostatic loading resulted in minimal chondrocyte death (5.8% ±4% at 0.5 MPa and 3.0% ±3% at 1.0MPa).

MnTMPyP has been shown to be a potent superoxide scavenger and Figure 5 shows that pre-treatment significantly reduced oxidant staining at both 0.5MPa (15.6%±10%) and 0.25MPa (4.8%±2%) compared to the untreated specimens at the same stress levels, indicating that superoxide is the primary ROS constituent in loading response observed in these experiments. The mitochondrial electron transport inhibitor, rotenone, significantly reduced oxidant staining at 0.25MPa (12.6% ±5%) static compression ($p<0.05$), but did not significantly reduce staining at 0.5MPa (42% ±19%), indicating that mitochondrial complex I plays a significant role in the superoxide release at lower stresses (Fig 5). Similar trends were observed when explants were pre-treated with cytochalasin B, an inhibitor of actin polymerization (Fig 5). DHE staining declined significantly (14% ±13%) at 0.25MPa ($p<0.05$), but no effect was observed at 0.5MPa (54.6% ±12%), showing that an intact cytoskeleton is required for ROS release at the lower stresses. Representative DHE images for each treatment can be found in the supplementary information (Fig S3).

4. Discussion

This study demonstrated that semi-confined static compressive stress induces superoxide release in cartilage chondrocytes in a strain-dependent manner. This response was similar to that observed in cartilage loaded cyclically over a similar range of compressive stresses (Tomiyama et al. 2007). However, ROS production under hydrostatic stress was negligible at 0.5MPa and 1.0MPa, indicating that tissue strain and/or distortion are required for the ROS response.

Treatment with rotenone reduced DHE staining under static stress compression by 65% in specimens loaded to 0.25 MPa, demonstrating that mitochondrial complex 1 (NADH dehydrogenase) is involved. These findings were in part consistent with our previous work demonstrating that injury-induced ROS increases were mitochondrial in origin (Goodwin et al. 2010). At the higher stresses/strains, additional sources, such as NADPH oxidase, which would not be inhibited by rotenone, may have contributed significantly to ROS levels, helping explain why a significant reduction was not seen at 0.5MPa, though this is speculative and warrants further investigation.

Similar to rotenone, cytochalasin B pre-treatment resulted in a 61% reduction in oxidant production in specimens loaded at 0.25 MPa, but not at 0.5 MPa. Previous studies have demonstrated that the cytoskeleton facilitates transduction of tissue-level forces to cell-level strains that are communicated to intracellular organelles and the nucleus (Orr et al. 2006; Knight et al. 2006). Removing these intracellular communication connections could explain the decrease in mitochondrial oxidant production at lower stresses. This idea is bolstered by the low level of DHE staining in hydrostatically stressed explants. A previous impact injury model demonstrated that cytoskeletal dissolution prior to impact injury significantly reduced impact-related increases in ROS and chondrocyte death (Sauter et al. 2012), which agrees with our findings at lower stress levels. However, at the higher compressive stress level (0.5

MPa), the data from this experiment point toward other sources of ROS which were not affected by cytoskeletal dissolution. Alternatively, cytochalasin D is known to reduce chondrocyte stiffness (Trickey et al. 2004), which could lead to higher cell strain and negate any intracellular benefit from dissolving intracellular attachments to reduce ROS levels at this higher stress.

To confirm if superoxide was the main ROS constituent, MnTMPyP was added to the culture medium prior to loading. MnTMPyP works as an ion superoxide oxireductase that reduces superoxide to hydrogen peroxide only after it has been reduced by intracellular NADPH and GSH (Araujo-Chaves et al. 2011; Peshavariya et al. 2007). As such, it is useful for blocking superoxide production in short term experiments, but would pose a problem in longer term experiments where MnTMPyP could deplete the reducing pool of NADPH and GSH, leading to an increase of intracellular oxidant levels from hydrogen peroxide buildup (Araujo-Chaves et al. 2011; Gardner et al. 1996). Here, MnTMPyP treatment reduced DHE staining by 87% at 0.5MPa and by 72% at 0.25MPa.

While this study clearly demonstrates a relationship between ROS release and tissue strain, it has several limitations. Firstly, the loading regimen is not physiological (one hour static loading) leading to sustained axial strains that in most cases were greater than what would be found *in vivo*. Typical *in vivo* contact deformation in the knee on the medial and lateral cartilage were measured at 12.1% and 14.6%, respectively, after 300 seconds of full body weight static loading (Hosseini et al. 2010) and in a weight-bearing single leg lunge, deformations in the knee will reach 30% (Bingham et al. 2008). Also, only the superficial zone was imaged, which is found to be softer than the underlying zones (Buckley et al. 2008; Schinagl et al. 1996) and shows higher local strains relative to rest of the tissue (Chahine et al. 2007). The duration of stress application and time point of confocal imaging were both fixed in these experiments, leaving the effects of shorter or longer stress durations and differing confocal time points unknown. As such the long-term viability of the explants in these treatments is also unknown. We would expect that cell death and DHE signals would be exacerbated under longer duration stress application, and that cell death would continue to rise at later time points, but this remains to be tested directly. Ideally this response would be verified with an intact joint, under physiological cyclic loading to allow for fluid permeability and a natural cartilage-on-cartilage contact surface, which would overcome the limitation of an impermeable rigid indenter.

While these shortcomings make extrapolating the findings in this experiment to *in vivo* conditions difficult, the experiment does effectively demonstrate that the amounts of ROS production and chondrocyte death are predictable by axial-tissue strain in a mechanically stressed explant culture system.

Mitochondrial oxidants, once thought to be primarily pathological, participate in multiple physiological processes and are now widely recognized for their primary role in intracellular signaling, especially in highly oxygenated tissues (Hamanaka and Chandel 2010). Interestingly, mitochondrial oxidants help stabilize hypoxia inducible transcription (Hif) factors in response to tissue hypoxia (Bell et al. 2007; Weidemann and Johnson 2008). This sensitivity to hypoxia suggests an important role for mitochondrial in cartilage physiology,

where the tissue is inherently hypoxic. Also, previous work showed that 100μM tertiary butyl hydroperoxide (tBHP) treatments induced glycolytic activity in cartilage, increasing Hif-1α and GAPDH expression (Ramakrishnan et al. 2010). In addition, catabolic processes including cyclooxygenase stimulation and matrix metalloproteinase 13 (MMP-13) activity is seen to increase in response to ROS (Cillero-Pastor et al. 2008; Ahmad et al. 2011). While progress on understanding the roles of mitochondrial ROS is underway, there is still much to be elucidated.

In conclusion, the results of this investigation show that mechanical deformation of cartilage explant induces strain-dependent superoxide release. This superoxide release is dependent on mechanical distortion, which at lower strains requires an intact cytoskeletal network to induce mitochondrial superoxide release. This strain-dependent release of superoxide may be relevant to the observation that physiological mechanical stresses are beneficial to cartilage health and increase biosynthetic activity. As an avascular tissue, with oxygen level estimates ranging from 1% to 6% (Zhou et al. 2004), cartilage depends primarily on glycolysis for ATP production (Lee and Urban 1997). However, when cartilage is under completely anoxic conditions, glycolytic activity declines sharply, a response termed the *negative Pasteur effect* (Lee and Urban 1997, 2002). Interestingly, the hypoxia-induced inhibition can be reversed by providing exogenous oxidants such as methylene blue (Lee and Urban 2002). Mitochondrial oxidants also have a key role in maintaining glycolysis in this low oxygen environment. When mitochondrial ROS are blocked, cartilage ATP production drops, but can be rescued by the addition of external tBPH (Martin et al. 2012). The ROS produced by mitochondria in response to normal mechanical stress act in a similar manner to support glycolysis, and upon their removal drastically reduce ATP levels in cartilage (Wolff et al. 2013). Additional studies on the effects of oxidants and mechanical stresses on ATP production and cartilage homeostasis are needed to further elucidate the connections.

Supplementary Material

Refer to Web version on PubMed Central for supplementary material.

Acknowledgments

We thank Rachel Brouillette for editing. Confocal images were all taken at the Central Microscopy Research Facility, University of Iowa, Iowa City. This work was supported by the National Institutes of Health (CORT NIH P50 AR055533), and by a Merit Review Award from the Department of Veterans Affairs.

References

Ahmad R, Sylvester J, Ahmad M, Zafarullah M. Involvement of H-Ras and reactive oxygen species in proinflammatory cytokine-induced matrix metalloproteinase-13 expression in human articular chondrocytes. Arch Biochem Biophys. 2011; 507(2):350–355.10.1016/j.abb.2010.12.032 [PubMed: 21211511]

Araujo-Chaves JC, Yokomizo CH, Kawai C, Mugnol KC, Prieto T, Nascimento OR, Nantes IL. Towards the mechanisms involved in the antioxidant action of MnIII [meso-tetrakis(4-N- methyl pyridinium) porphyrin] in mitochondria. Journal of bioenergetics and biomembranes. 2011; 43(6): 663–671.10.1007/s10863-011-9382-3 [PubMed: 21986957]

Bachrach NM, Mow VC, Guilak F. Incompressibility of the solid matrix of articular cartilage under high hydrostatic pressures. Journal of Biomechanics. 1998; 31(5):445–451. http://dx.doi.org/10.1016/S0021-9290(98)00035-9. [PubMed: 9727342]

Bell EL, Klimova TA, Eisenbart J, Schumacker PT, Chandel NS. Mitochondrial reactive oxygen species trigger hypoxia-inducible factor-dependent extension of the replicative life span during hypoxia. Molecular and cellular biology. 2007; 27(16):5737–5745.10.1128/MCB.02265-06 [PubMed: 17562866]

Bingham JT, Papannagari R, Van de Velde SK, Gross C, Gill TJ, Felson DT, Rubash HE, Li G. In vivo cartilage contact deformation in the healthy human tibiofemoral joint. Rheumatology (Oxford). 2008; 47(11):1622–1627.10.1093/rheumatology/ken345 [PubMed: 18775967]

Blanco FJ, Rego I, Ruiz-Romero C. The role of mitochondria in osteoarthritis. Nat Rev Rheumatol. 2011; 7(3):161–169.10.1038/nrrheum.2010.213 [PubMed: 21200395]

Buckley MR, Gleghorn JP, Bonassar LJ, Cohen I. Mapping the depth dependence of shear properties in articular cartilage. J Biomech. 2008; 41(11):2430–2437.10.1016/j.jbiomech.2008.05.021 [PubMed: 18619596]

Chahine NO, Ateshian GA, Hung CT. The effect of finite compressive strain on chondrocyte viability in statically loaded bovine articular cartilage. Biomech Model Mechanobiol. 2007; 6(1-2):103–111.10.1007/s10237-006-0041-2 [PubMed: 16821016]

Chance B, Williams GR. Respiratory enzymes in oxidative phosphorylation. I. Kinetics of oxygen utilization. J Biol Chem. 1955; 217(1):383–393. [PubMed: 13271402]

Cillero-Pastor B, Carames B, Lires-Dean M, Vaamonde-Garcia C, Blanco FJ, Lopez-Armada MJ. Mitochondrial dysfunction activates cyclooxygenase 2 expression in cultured normal human chondrocytes. Arthritis Rheum. 2008; 58(8):2409–2419.10.1002/art.23644 [PubMed: 18668543]

Durrant LA, Archer CW, Benjamin M, Ralphs JR. Organisation of the chondrocyte cytoskeleton and its response to changing mechanical conditions in organ culture. J Anat. 1999; 194(Pt 3):343–353. [PubMed: 10386772]

Gardner PR, Nguyen DD, White CW. Superoxide scavenging by Mn(II/III) tetrakis (1-methyl-4-pyridyl) porphyrin in mammalian cells. Arch Biochem Biophys. 1996; 325(1):20–28.10.1006/abbi.1996.0003 [PubMed: 8554339]

Goodwin W, McCabe D, Sauter E, Reese E, Walter M, Buckwalter JA, Martin JA. Rotenone prevents impact-induced chondrocyte death. J Orthop Res. 2010; 28(8):1057–1063.10.1002/jor.21091 [PubMed: 20108345]

Hamanaka RB, Chandel NS. Mitochondrial reactive oxygen species regulate cellular signaling and dictate biological outcomes. Trends Biochem Sci. 2010; 35(9):505–513.10.1016/j.tibs.2010.04.002 [PubMed: 20430626]

Hosseini A, Van de Velde SK, Kozanek M, Gill TJ, Grodzinsky AJ, Rubash HE, Li G. In-vivo time-dependent articular cartilage contact behavior of the tibiofemoral joint. Osteoarthritis Cartilage. 2010; 18(7):909–916.10.1016/j.joca.2010.04.011 [PubMed: 20434573]

Knight MM, Bomzon Z, Kimmel E, Sharma AM, Lee DA, Bader DL. Chondrocyte deformation induces mitochondrial distortion and heterogeneous intracellular strain fields. Biomech Model Mechanobiol. 2006; 5(2-3):180–191. [PubMed: 16520962]

Lee RB, Urban JP. Evidence for a negative Pasteur effect in articular cartilage. Biochem J. 1997; 321(Pt 1):95–102. [PubMed: 9003406]

Lee RB, Urban JP. Functional replacement of oxygen by other oxidants in articular cartilage. Arthritis Rheum. 2002; 46(12):3190–3200.10.1002/art.10686 [PubMed: 12483723]

Martin JA, Martini A, Molinari A, Morgan W, Ramalingam W, Buckwalter JA, McKinley TO. Mitochondrial electron transport and glycolysis are coupled in articular cartilage. Osteoarthritis Cartilage. 2012; 20(4):323–329.10.1016/j.joca.2012.01.003 [PubMed: 22305999]

Martin JA, McCabe D, Walter M, Buckwalter JA, McKinley TO. N-acetylcysteine inhibits post-impact chondrocyte death in osteochondral explants. The Journal of bone and joint surgery American volume. 2009; 91(8):1890–1897.10.2106/JBJS.H.00545 [PubMed: 19651946]

Orr AW, Helmke BP, Blackman BR, Schwartz MA. Mechanisms of mechanotransduction. Dev Cell. 2006; 10(1):11–20.10.1016/j.devcel.2005.12.006 [PubMed: 16399074]

Otte P. Basic cell metabolism of articular cartilage. Manometric studies. Zeitschrift fur Rheumatologie. 1991; 50(5):304–312. [PubMed: 1776367]

Peshavariya HM, Dusting GJ, Selemidis S. Analysis of dihydroethidium fluorescence for the detection of intracellular and extracellular superoxide produced by NADPH oxidase. Free radical research. 2007; 41(6):699–712.10.1080/10715760701297354 [PubMed: 17516243]

Quinn TM, Grodzinsky AJ, Buschmann MD, Kim YJ, Hunziker EB. Mechanical compression alters proteoglycan deposition and matrix deformation around individual cells in cartilage explants. J Cell Sci. 1998; 111(Pt 5):573–583. [PubMed: 9454731]

Quinn TM, Morel V, Meister JJ. Static compression of articular cartilage can reduce solute diffusivity and partitioning: implications for the chondrocyte biological response. J Biomech. 2001; 34(11): 1463–1469. [PubMed: 11672721]

Ramakrishnan P, Hecht BA, Pedersen DR, Lavery MR, Maynard J, Buckwalter JA, Martin JA. Oxidant conditioning protects cartilage from mechanically induced damage. J Orthop Res. 2010; 28(7):914–920.10.1002/jor.21072 [PubMed: 20058262]

Ramakrishnan PS, Pedersen DR, Stroud NJ, McCabe DJ, Martin JA. Repeated measurement of mechanical properties in viable osteochondral explants following a single blunt impact injury. Proceedings of the Institution of Mechanical Engineers Part H, Journal of engineering in medicine. 2011; 225(10):993–1002.

Sauter E, Buckwalter JA, McKinley TO, Martin JA. Cytoskeletal dissolution blocks oxidant release and cell death in injured cartilage. J Orthop Res. 2012; 30(4):593–598.10.1002/jor.21552 [PubMed: 21928429]

Schinagl RM, Ting MK, Price JH, Sah RL. Video microscopy to quantitate the inhomogeneous equilibrium strain within articular cartilage during confined compression. Annals of biomedical engineering. 1996; 24(4):500–512. [PubMed: 8841725]

Stevens AL, Wishnok JS, White FM, Grodzinsky AJ, Tannenbaum SR. Mechanical injury and cytokines cause loss of cartilage integrity and upregulate proteins associated with catabolism, immunity, inflammation, and repair. Mol Cell Proteomics. 2009; 8(7):1475–1489.10.1074/mcp.M800181-MCP200 [PubMed: 19196708]

Stockwell RA. Morphometry of cytoplasmic components of mammalian articular chondrocytes and corneal keratocytes: species and zonal variations of mitochondria in relation to nutrition. J Anat. 1991; 175:251–261. [PubMed: 2050570]

Strathmann J, Klimo K, Sauer SW, Okun JG, Prehn JH, Gerhauser C. Xanthohumol-induced transient superoxide anion radical formation triggers cancer cells into apoptosis via a mitochondria-mediated mechanism. FASEB journal : official publication of the Federation of American Societies for Experimental Biology. 2010; 24(8):2938–2950.10.1096/fj.10-155846 [PubMed: 20335224]

Tomiyama T, Fukuda K, Yamazaki K, Hashimoto K, Ueda H, Mori S, Hamanishi C. Cyclic compression loaded on cartilage explants enhances the production of reactive oxygen species. The Journal of rheumatology. 2007; 34(3):556–562. [PubMed: 17309123]

Torzilli PA, Deng XH, Ramcharan M. Effect of compressive strain on cell viability in statically loaded articular cartilage. Biomech Model Mechanobiol. 2006; 5(2-3):123–132.10.1007/s10237-006-0030-5 [PubMed: 16506016]

Trickey WR, Vail TP, Guilak F. The role of the cytoskeleton in the viscoelastic properties of human articular chondrocytes. J Orthop Res. 2004; 22(1):131–139.10.1016/S0736-0266(03)00150-5 [PubMed: 14656671]

Weidemann A, Johnson RS. Biology of HIF-1alpha. Cell death and differentiation. 2008; 15(4):621–627.10.1038/cdd.2008.12 [PubMed: 18259201]

Wolff KJ, Ramakrishnan PS, Brouillette MJ, Journot BJ, McKinley TO, Buckwalter JA, Martin JA. Mechanical stress and ATP synthesis are coupled by mitochondrial oxidants in articular cartilage. J Orthop Res. 2013; 31(2):191–196.10.1002/jor.22223 [PubMed: 22930474]

Wong M, Carter DR. Articular cartilage functional histomorphology and mechanobiology: a research perspective. Bone. 2003; 33(1):1–13. S8756328203000838 [pii]. [PubMed: 12919695]

Zhou S, Cui Z, Urban JP. Factors influencing the oxygen concentration gradient from the synovial surface of articular cartilage to the cartilage-bone interface: a modeling study. Arthritis Rheum. 2004; 50(12):3915–3924.10.1002/art.20675 [PubMed: 15593204]

Abbreviations

ROS	Reactive oxygen species
DHE	Dihydroethidium
MPa	Megapascal
MnTMPyP	Mn(III)tetrakis (1-methyl-4-pyridyl) porphyrin pentachloride
EthD-2	Ethidium homodimer-2
QCIP™	Quantitative Cell Image Processing
Hif	Hypoxia inducible transcription
tBHP	Tertiary butyl hydroperoxide
MMP-13	Matrix metalloproteinase 13

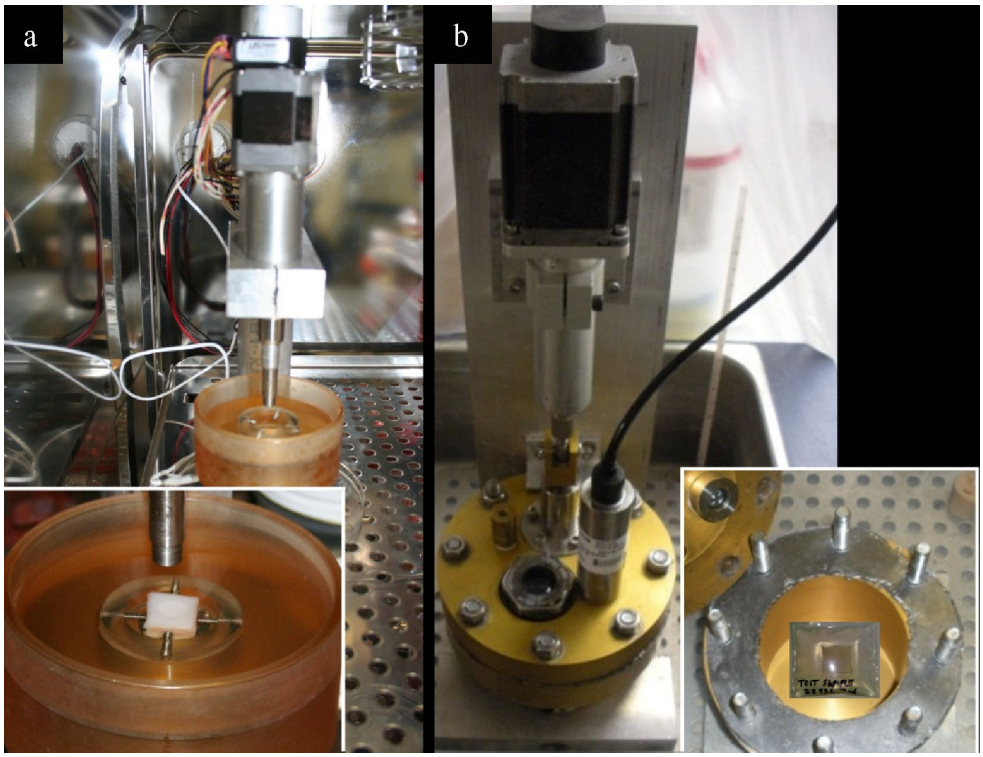

Figure 1.

Mechanical loading devices. (a) Device for static compressive stress shown in a low oxygen incubator. The inset shows an osteochondral explant submerged in culture medium in the housing under the indenter. (b) Hydrostatic device shown in a water bath. The inset shows an explant sealed in a plastic bag containing culture medium. The bag is submerged under water in the unit.

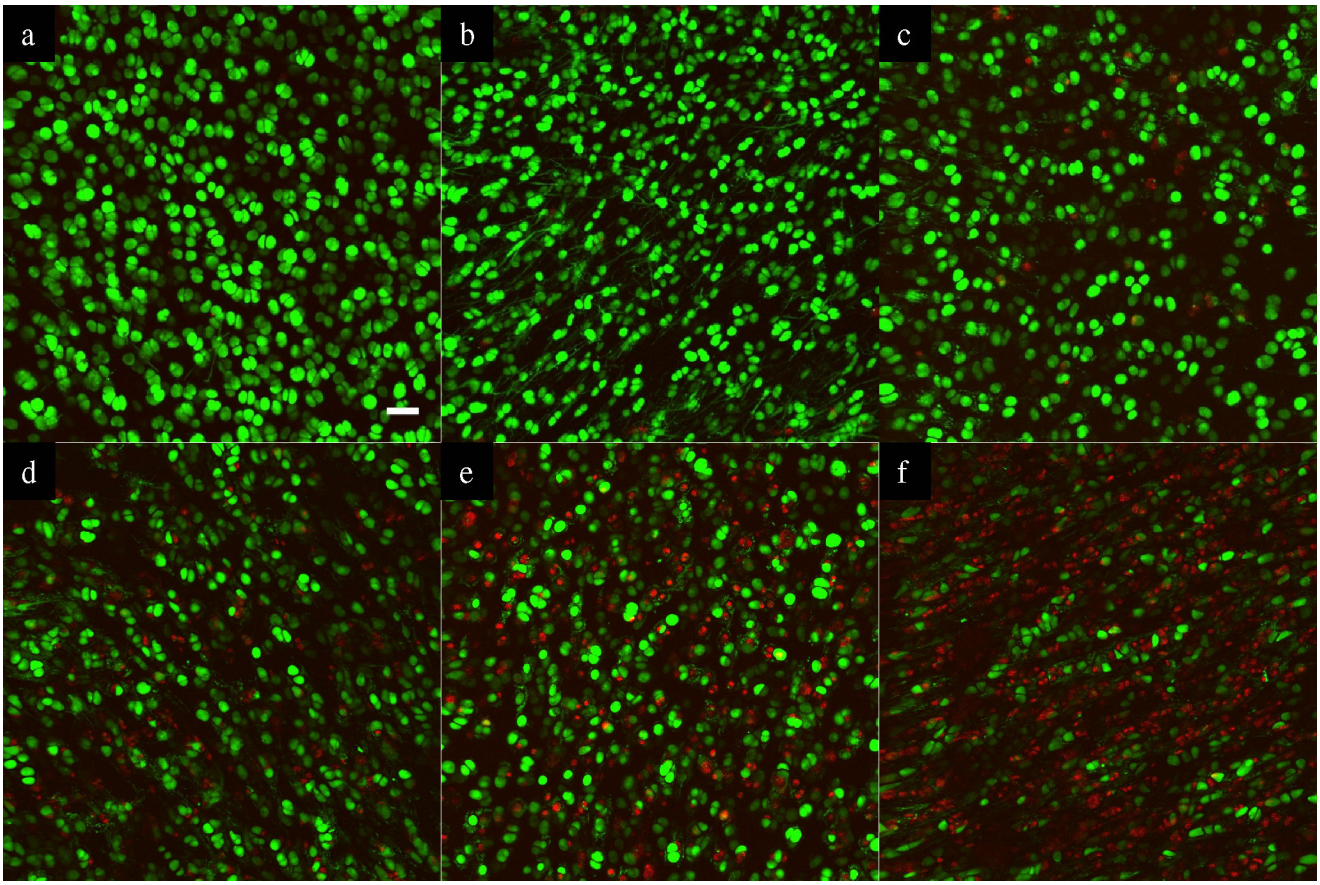

Figure 2.

Representative z-axis stacked confocal images (20× objective) showing oxidant production (Red) and live cells (Green) after static compressive stress with 0 MPa (a), 0.05MPa (b), 0.1 MPa (c), 0.25 MPa (d), 0.5 MPa (e), and 1.0 MPa (f). The white bar indicates 40 microns.

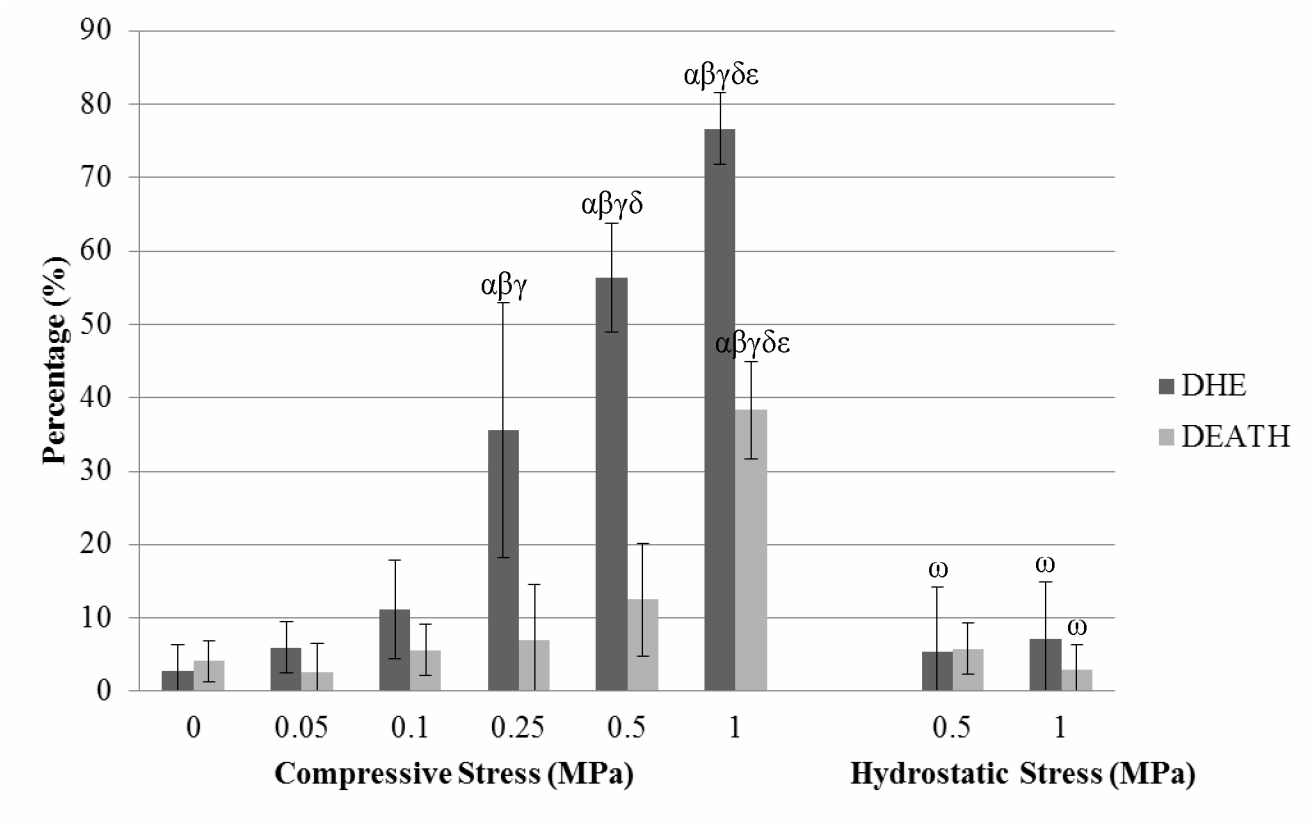

Figure 3.

Percentage of cells stained with oxidative marker, dihydroethidium (DHE), and cell death marker, EthD-2 (DEATH), under various static stresses. Statistical significance markers are denoted ($p<0.05$) as α indicating significance vs. unloaded control, β vs. 0.05MPa, γ vs. 0.1MPa, δ vs. 0.25MPa, and ε vs. 0.5MPa for compressive stress. For hydrostatic stress, ω represents significance compared to the corresponding compressive stress and stain.

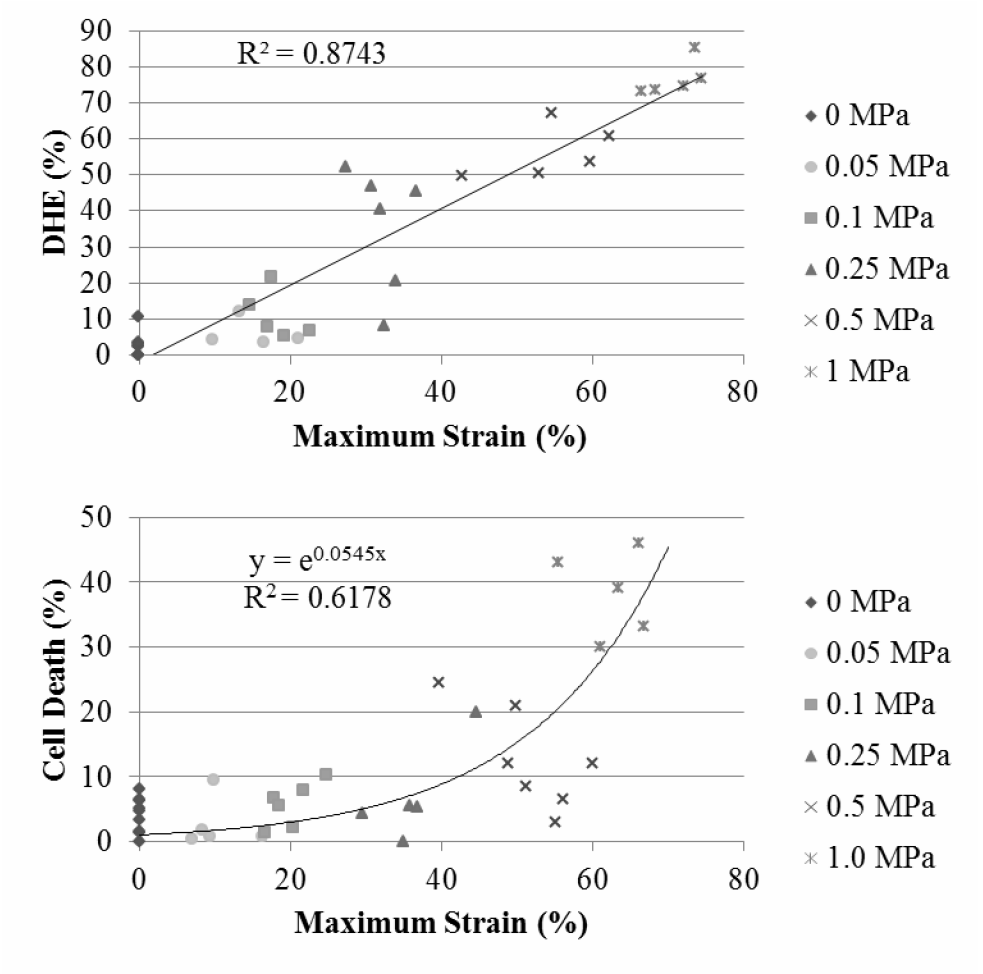

Figure 4.

DHE staining and bulk tissue strain after stress completion (a). Regression analysis revealed a strong linear relationship between DHE and strain. Cell death and bulk tissue strain (b). Each point represents the mean percentage from the three image sites of each explant.

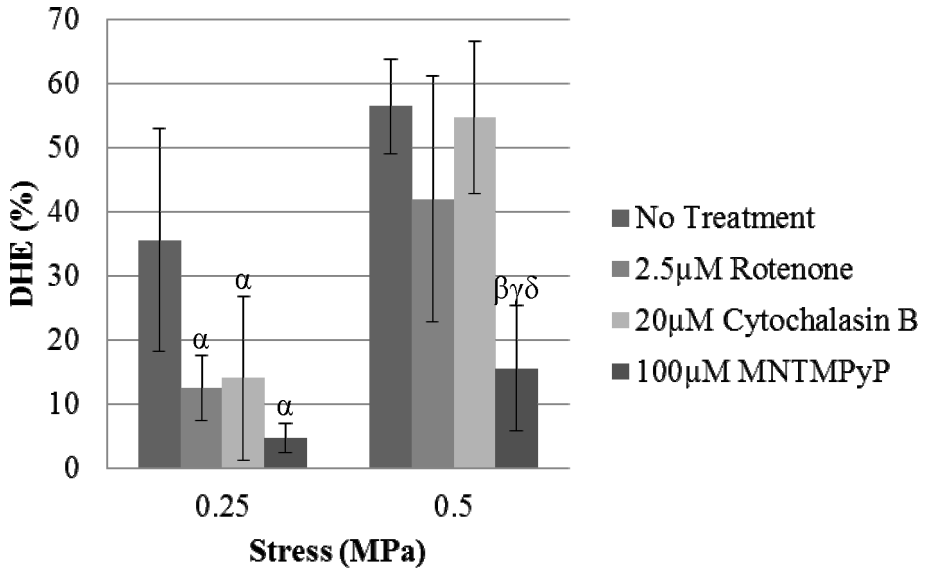

Figure 5.

Effects of MnTMPyP, rotenone, and cytochalasin B on stress-induced DHE staining. Sequestering superoxide produced significant reductions in DHE staining at both 0.5MPa and 0.25MPa ($p<0.05$). Inhibition of mitochondrial electron transport with rotenone decreased DHE staining after 1 hour of 0.25MPa static compressive stress ($p<0.05$). Cytoskeletal dissolution with cytochalasin B significantly decreased DHE staining at 0.25MPa ($p<0.05$). Statistical significance markers ($p<0.05$) are denoted as α indicating significance vs. 0.25MPa untreated specimens, β vs. 0.5MPa untreated specimens, γ vs. 0.5MPa rotenone treatment, and δ vs. 0.5MPa cytochalasin B treated.